MCFC integrated system in a biodiesel production process

F. Urbani, S. Freni*, A. Galvagno, V. Chiodo

CNR-ITAE "Nicola Giordano", Via S. Lucia sopra Contesse, 5 98126 Messina, Italy

ARTICLE INFO

ABSTRACT

The continuous increasing in biodiesel production by transesterification process is leading to an excess of glycerol production as a byproduct.

The utilization of this huge amount of glycerol appears as a not easy solvable problem and thus several authors have proposed alternative ways.

The integration of the main production process with a glycerol feed molten carbonate fuel cells bottoming cycle, to satisfy plant energy requirements, seems to be one of the most promising one.

The proposed paper reports the main results obtained by authors in the framework of an investigation on a possible use of glycerol as energy sources for a real pilot plant for biodiesel production.

An overall evaluation of worldwide biodiesel production plants was made and especially about the production capacity in European Union in the last decade. To make a more detailed study, authors were taken into account a real production plant.

After a preliminary step, purported to plant mass and energy flows determination, authors considered the integration of a bottoming cycle based on: (i) steam reforming of glycerol for syn-gas production; (ii) molten carbonate fuel cells (MCFC) system supplied by syn-gas for heat and electricity production.

A mathematical model, based on experimental data, has been developed to calculate mass and energy balances for the proposed plant lay-out as well as plant energy efficiency enhancement has been determined.

Results have evidenced the feasibility of this process and demonstrated that plant integrated with bottoming cycle can reach a very high level of energy self-production.

© 2010 Elsevier B.V. All rights reserved.

1. Introduction

Now days, it is well known technology evolution and energy sources availability are two key factors for human society development.

During the last century, the research of new energy sources it has, mainly, been confined to the exploration for new fossil hydrocarbons wells. Some severe problems arose due to the massive combustion of fossil hydrocarbons utilized to energy production. Global warming due to greenhouse gas emission and local pollution due to cars exhaust emissions are two of the most alarming factors that are taking up extensive research efforts to be attenuated.

In this aim, a lot of researchers are investigating new technologies to reduce the use of fossil hydrocarbons by increasing the production of fuels derived from vegetables biomasses.

In this field, one of the most promising technology concerns the production of biodiesel from vegetable oils. This process is based on the transesterification of oils with a treatment that requires methanol, steam and electricity with some additional chemicals

as sodium hydroxide, chlorum hydride, etc. [1]. Biodiesel is main product of this process and a mixture of glycerol and water (80/20, wt.%) is generated as by-product. The amount of glycerol is a significant rate if compared to the biodiesel mass production. As example, it is required a mass of 1037 kg of vegetable oil, 105 MJ of electricity and 1373 MJ for steam to produce 1000 kg of biodiesel with 170 kg of glycerol as byproduct. Thus, the mass rate of glycerol production is almost 17% of biodiesel one and it can not be considered negligible in the framework of the overall process balance.

Several commercial utilizations [2,3] have been proposed for glycerol produced in biodiesel plants. Among these, one promising way concerns to integrate the main production process with a glycerol feed bottoming cycle to produce electricity and heat. Electrochemical devices like solid oxide fuel cells [4,5] or molten carbonate fuel cells [6,7] seem to be appropriate for this purpose.

Since the last decade, CNR-ITAE's researchers developed a wide experience on syn-gas production from several raw fuels [8,10]. Based on this preview activity, the authors considered the possibility to use the glycerol to supply a bottom co-generation cycle integrated with the main diesel production process. This study started from the experimental evidence that glycerol can be catalytically reformed to produce hydrogen rich gas mixture having

---

* Corresponding author. Tel.: +39 090 624230; fax: +39 090 624247.
  E-mail address: salvatore.freni@itae.cnr.it (S. Freni).

good characteristics to be used as fuel for a molten carbonate fuel cells.

Thus, authors efforts have been addressed to demonstrate the feasibility of a biodiesel production plant composed by three steps: (1) diesel production from vegetable oils; (2) syn-gas production from glycerol steam reforming; (3) bottoming cycle based on molten carbonate fuel cells technology.

The results reported in this paper have demonstrated the technological feasibility of this application as well as energy balance of the production cycle can be useful advantaged by recycling energy/heat and steam released by the MCFC bottoming cycle.

2. Biodiesel market development

Biodiesel production have recorded an enormous growth in the last decade. The main drivers of this increase are the reducing dependence on imported oil and the reducing of greenhouse gas emission. Compared to diesel, the bio-fuel can be used in existing diesel engines without considerable modifications and it is compatible with existing fuel distribution infrastructure [11]. The European Union (EU) is world leader in production (67.9%) and consumption of biodiesel, followed by United States (17.8%) and Brazil [12]. The EU leadership is determined by the partial or total exemption of bio-fuels from taxes, which affect the price of traditional fuels. [13].

Fig. 1 shows the comparison between potential plant production capacity and real production of biodiesel in the EU member states. It may be noted that in 2005 and 2006 capacity and production are very close, while from 2007 the growth trend of plants was not followed by a marked increase in biodiesel production. So the present trend is characterized by a faster growth of capacity than the actual production and marketing of biodiesel. The statistics for 2008 (Table 1) and 2009 shows that about 50% of existing plants in EU remains inactive. The international competition that has established in recent years has been the main driver of this trend. In March 2009 European Union imposed anti-dumping and countervailing measures against U.S. biodiesel for the next 5 years, by adopting tough measures against unfair trade practice that violates fundamental principles of WTO (World Trade Organization).
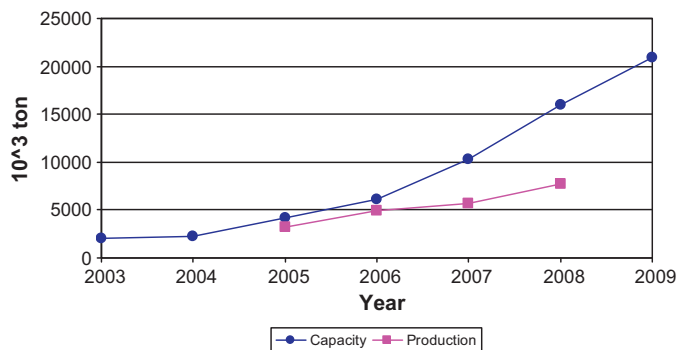

Fig. 1. Development of capacity and production in recent years in EU (source European Biodiesel Board).

Table 1
Capacity vs production in EU in 2008 (source European Biodiesel Board).

	Capacity (kton)	Production (kton)	Prod./Cap. (%)
Germany	5302	2819	53
France	1980	1815	92
Italy	1566	595	38
Spain	1267	207	16
U.K.	726	192	26
Belgium	665	277	42
Others EU states	4493	1850	41
Total	15,999	7755	48

This decision will help restore the legitimate rights of EU producers to operate in conditions of fairness [14].

2.1. Overview of biodiesel production process

In this paragraph is described the biodiesel production process, taking into account the design of the transesterification plant based on a commercial facility located in Kansas City (MO), with a production of 10,504 kg h^{-1} of biodiesel [1]. The core of the transformation process for soybean oil in biodiesel, is determined by a reaction known as transesterification. This reaction is an ester conversion
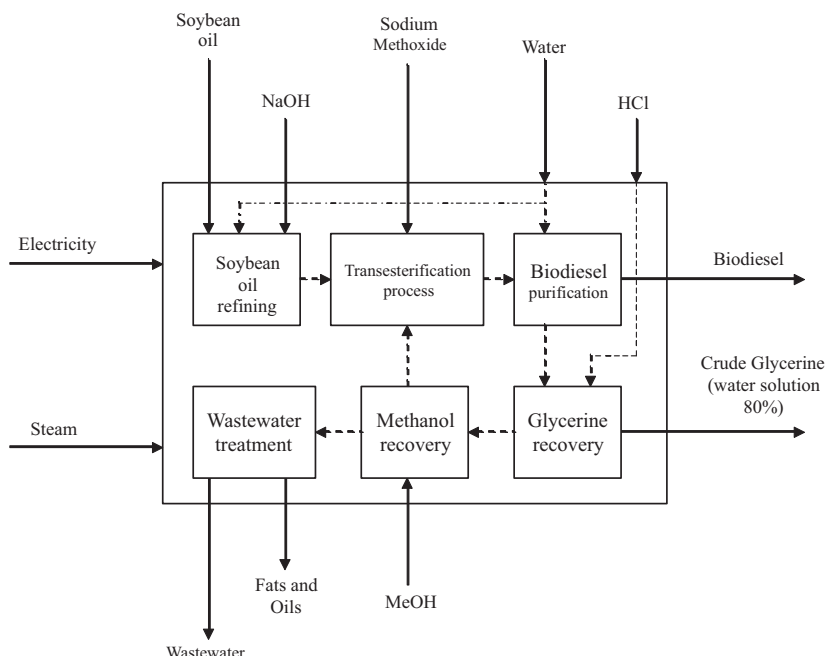

Fig. 2. Model plant of biodiesel process.

		Input	Output
Material	Crude soybean oil	10,897 kg h^{-1}	
	Sodium methoxide	252 kg h^{-1}	
	Sodium hydroxide (9.5%)	253 kg h^{-1}	
	Hydrochloric acid (10%)	792 kg h^{-1}	
	Methanol	940 kg h^{-1}	
	Water	3738 kg h^{-1}	
Energy	Electricity	303.6 kW	
	For steam	14,422 MJ h^{-1}	
Product	Biodiesel	–	10,504 kg h^{-1}
	Crude glycerine	–	2235 kg h^{-1}
	Oil and grease	–	129 kg h^{-1}
	Total wastewater	–	4004 kg h^{-1}

process which splits up triglycerides of soybean oil, replacing the glycerol of triglycerides with alkyl radical of the alcohol used. The reaction occurs through the introduction of a catalyst. As known from the transesterification reaction three moles of fatty acid alkyl monoester (biodiesel) and a mole of glycerol are obtained from three moles of alcohol are used per mole of triglyceride at low temperatures ($\approx$340 K) and at modest overpressure (2 bar). Although the theoretical molar ratio is 3:1, a greater molar ratio is generally used to shift the equilibrium to the products side. Through transesterification, high viscosity is reduced to a value closer to diesel fossil fuel while cetane number and heating value are saved [12,14,15].

In Fig. 2 is shown the model plant broken out into the six main processing sections. Soybean oil received from the crushing operation is introduced in the first process section to remove, through a caustic refining, free fatty acids. Before sending to the second section, the transesterification reactor, the water into the oil, which can be harmful for the reactors, has to be removed. In this plant section the refined soybean oil is combined with an excess of methanol and catalyst. This reaction produces biodiesel and glycerine. The first product is sent to the "biodiesel purification" section, in which biodiesel is separated, through a process of washing and drying, from glycerine, methanol and other water-soluble components. The second one is sent to the "glycerine recovery" module, where glycerine rich streams from transesterification settlers, ester purification and ester dryer condensate are collected, heated, and fed to the glycerine distillation. The output of this section of the plant is crude glycerine, a water solution with 80% of glycerol, nowadays sold as a by-product.

Methanol and steam from the glycerine purification are sent to "methanol recovery" section, a distillation column where methanol is separated from the waste components to be reused in the process of transesterification. In the "wastewater treatment", wastes collected from all the others section of the process are sent to clarifiers for removal of oil and grease. The oil and grease are skimmed off and sent to land filled, the remaining wastewater is sent to the municipal sewer system [16].

Table 2 shows input and output necessary to Kansas City plant for methyl ester production to produce a biodiesel flow of about 10,500 kg h^{-1}.

For every 10,500 kg of biodiesel produced, 10,897 kg of soybean oil are required as feedstock and approximately 940 kg of methanol is added to the system, twice the required stoichiometric ratio. Only 26% of methanol introduced is involved in the reaction, while the remainder is recovered. Hydrochloric acid (HCl) is required in "glycerine recovery" section to acidulate glycerine.

Output of the process are, as main products, about 10,500 kg of biodiesel and 2235 kg of crude glycerine, as wastage oils, grease and wastewater; energy requirements concern 303.6 kW of electric power and 14,422 MJ h^{-1} of thermal power to steam generation.

3. Glycerol steam reforming

Steam reforming must be carried out at high temperatures, low pressure and high steam carbon ratio by different kind of feedstocks [17]. Overall, the reaction of glycerol steam reforming can be given as follows:

$$C_3H_8O_3 + 3H_2O \rightarrow 7H_2 + 3CO_2 \quad (\Delta H^0_{298} = +346.4 \text{ kJ mol}^{-1}) \quad (1)$$
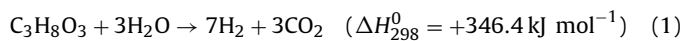
Thermodynamically, Eq. (1) is highly endothermic, therefore thermodynamic studies are very important to provide data on conditions that are conducive to hydrogen production. From literature it is known that the best conditions for producing hydrogen by glycerol are: temperature over 900 K, atmospheric pressure, and water/glycerol molar ratio of 9:1. Under these conditions methane production is minimized and carbon formation is thermodynamically inhibited [18–21].

Therefore, in order to investigate on the feasibility of hydrogen production through steam reforming of glycerol coming from biodiesel production process and use it in a fuel cell system, the thermodynamic equilibrium composition of the system containing $C_3H_8O_3$, H_2O, CO, CO_2, H_2 and CH_4 as a function of temperature were investigated by Mathematica® software. Subsequently, glycerol steam reforming reaction in terms of conversion and outlet stream composition were experimentally evaluated. Experimental data and thermodynamic values have been obtained as later described.

3.1. Experimental conditions

On the basis of our earlier experience, the most suitable steam reforming catalyst is rhodium based one [4,6–10]. Thus, several samples of 5 wt.% Rh/Al$_2$O$_3$, surface area (BET) of 163 m^2 g^{-1}, were prepared by impregnation (incipient wetness) using γ-Al$_2$O$_3$ AKZO-NOBEL 001-3P as carrier and a RhCl$_3$ aqueous solution. Therefore, the samples were dried at 353 K for 24 h and then air treated at 673 K for 12 h; subsequently, samples were pressed at 400 bar, crushed, sieved and only 40–70 mesh fraction was used for the catalytic tests.

Catalytic glycerol steam reforming experiments have been carried out on CNR ITAE apparatus lab-scale. This plant has been optimized along 15 years of investigation in the sector of organic oxygenates compound steam reforming [6–10]. Experiments have been performed on Rh/Al$_2$O$_3$ catalysts at high temperatures (823 K and 923 K), 1 bar of pressure and steam/carbon value about 3 mol mol^{-1}. A fixed-bed linear quartz micro-reactor (i.d. = 4 mm, h_{bed} = 10–20 mm), designed with a property geometry to avoid thermal decompositions of reactants, was filled with 0.02 g of catalyst diluted with 200 mg of similar sized inert material (SiC). The catalyst was reduced "in situ" at T = 923 K for 1 h under hydrogen flow, while a solution of anhydrous glycerol supplied by Sigma–Aldrich and water, was fed by an isocratic HP 1100 pump, vaporized at 573 K in a current of N$_2$. Before each test run, the vaporized water/glycerol mixture was on-line analyzed by gas chromatography HP Agilent 6890 (equipped with four columns: Molecular Sieve 5A, Porapack QS, Hysep Q, HP Innowax, and both TCD and FID detectors) in order to confirm that no cracking reaction products are generated under used experimental condition. Experiments were performed at gas hourly space velocity (GHSV) of 30,000 ml $_{C_3H_8O_3}$ h^{-1} ml$_{cat}^{-1}$. The total flow corresponding was 130 ml min^{-1} and the reaction stream composition was: 23.08 vol.% N$_2$; 69.23 vol.% H$_2$O; 7.69 vol.% C$_3$H$_8$O$_3$.

The outlet stream was cooled at 275 K and separated into liquid and gas phases. The gas phase was on-line analyzed by gas chromatography (HP Agilent 6890), while the liquid phase was analyzed by GC–MS (Agilent 5975C) provided with capillary column HP Innowax.

The catalytic performances were evaluated on the basis of equations system taking into account the total carbon balance [9]. The overall amount of coke deposited on the catalytic surface after each test run has been determined by CHNS elemental analysis of the discharged sample performed by a Carlo Erba Elemental Analyzer.

3.2. Thermodynamic aspects

The equilibrium composition of the system was calculated as a function of reaction temperature and steam to carbon (S/C) ratio, and it can be mathematically represented by a system of equations:

$$K_1 = \frac{x_{CO}^3 x_{H_2}^4}{x_{Gly} x_{H_2O}} p^5$$

$$K_2 = \frac{x_{CO_2} x_{H_2}}{x_{CO} x_{H_2O}}$$

$$K_3 = \frac{x_{CH_4} x_{H_2O}}{x_{CO} x^3} p^{-2}$$

where K_1, K_2 and K_3 represent the equilibrium constants. Respectively, x is the molar fractions of the gaseous components and P is the total pressure. The equilibrium are related to the free energies of each molecule involved in the equilibrium reactions and can be determined once the absolute temperature is specified. Furthermore, the reactions system can be summarized by following overall reaction:

$$C_aH_bO_c + mH_2O \rightarrow x_1CO + x_2CO_2 + x_3H_2O + x_4H_2 + x_5CH_4 \quad (2)$$
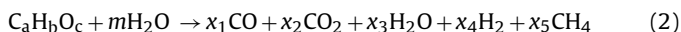
Therefore, equilibrium compositions have been calculated by solving the systems of non-linear equations formed by the equilibrium constant relationships and the mass balances according to Eq. (2) and corresponding to following expressions:

$$a = x_1 + x_2 + x_5$$

$$6a = 2x_3 + 2x_4 + 4x_5$$

$$2a = x_1 + 2x_2 + x_3$$

$$\frac{x_2 \times x_4}{x_1 \times x_3} = K_1$$

$$\frac{(x_1 / \sum x_i) \times (x_4 / \sum x_i)^3}{(x_3 / \sum x_i) \times (x_5 / \sum x_i)^3} = K_2$$

Because of the complexity of the analytical solution, a mathematical model based on an Mathematica® code has been used to solve these systems. The equilibrium constants were determined from thermodynamic data reported in literature [17], and in particular, the program requires the following as the input: (i) number of water mole, (ii) temperature, (iii) pressure; (iv) steam carbon ratio.

3.3. Experimental evidences

As previously reported, catalytic experiments were carried out exclusively to determine the most suitable operative conditions for hydrogen production by glycerol steam reforming. The experiments have been carried out by using commercial pure glycerol, nevertheless in our hypothetic plant there is available only 95 wt.% pure glycerol. This one has been considered by introducing a further glycerol purification step in the plant layout. Successively, an energetic evaluation of crude glycerine as fuel to supply a molten carbonate fuel cell was estimated. In this way, a comparison in
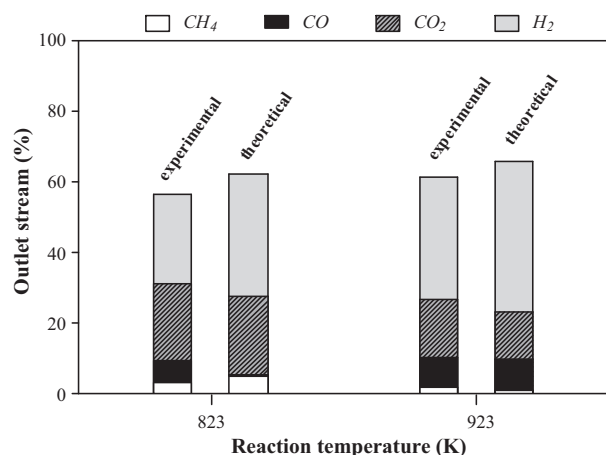

Fig. 3. Experimental and theoretical data of the outflow composition.

terms of dry gaseous products, at different temperatures by glycerol steam reforming, was carried out (see Fig. 3).

The glycerol conversion to primary products (H_2, CH_4, CO and CO_2) was measured 74% at 823 K and about 87% at 923 K, and in agreement to literature, it was found to increase with increasing temperature [10,18,19,22]. However, the conversion never reached values above 90%; this evidence could be attributed to the formation of other organic compounds such as acetone, acetaldehyde, ethanol, propanol, ethylene glycole, hydroxy-propane, which were detected into outlet liquid phase.

Fig. 3 depicts hydrogen production clearly increased with the temperature while the CH_4 presence decreased from 3.2 mol% at 823 K to 1.4 mol% at 923 K.

On the other hand, CO_2 concentration was found to be higher at 823 K (31 mol%), while CO production was found to be greater at higher temperature (10.22 mol%). On the whole, experimental results seem to be in respect of reaction pathway proposed for other oxygenated molecule [10,19], where the presence of the catalyst contributes with the temperature in the cleavage of C–C bonds. These last ones are accompanied by hydrogen evolution to form adsorbed carbon oxygenate on catalysts site, which further reacts with liquid water to release additional hydrogen and forms oxides of carbon. This suggests hydrogen production remains due to main reactions (WGS and methane reforming) and secondary reactions (dehydration, dehydrogenation) as appropriately considered in the thermodynamic calculations.

On line gas-chromatography analysis, both reagents and products, allowed to verify the carbon, hydrogen and oxygen balances. Results were very satisfactory, however, a modest carbon deposition on used catalysts, from 1.4 mg C $g_{cat}^{-1} \times$ h at 873 K to 2.2 mg C $g_{cat}^{-1} \times$ h at 923 K, was detected by CHNS elemental analysis after 15 h of test. This coke formation rate was considered negligible referred to contact time of the flow gas-input (0.12 s) on catalytic bed load (0.02 g). Moreover, the small coke formation observed by CHNS elemental analysis was mainly of whisker-like-structure [9] and only a little decay on stream has been observed.

On the basis of the experimental results, a thermodynamic analysis was performed in the same operative conditions. Hydrogen, CH_4, CO, CO_2, unreacted H_2O and $C_3H_8O_3$ have been considered as possible products from glycerol steam reforming. The main gaseous products concentrations have been calculated, at equilibrium composition, as a function of reaction temperature (823–923 K) and steam to carbon ratio ($S/C = 3$ mol mol^{-1}). These results, are also reported, on dry basis, in Fig. 3. As expected, the theoretical value of hydrogen molar fraction increases with the increasing of temperature and it appears higher than experimental ones both at 823 K
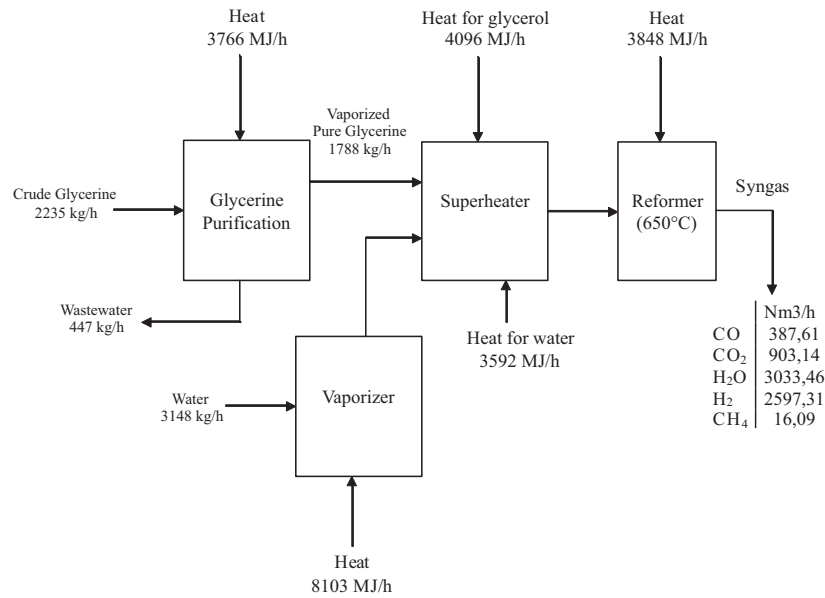
Fig. 4. Power and mass balance of the steam reforming process.

(62.17% vs 56.34%) and at 923 K (66.41% vs 61.84%), in according to thermodynamic of the reaction. As expected, the CH_4 production (0.5 mol%) resulted very poor at 923 K. This can be attributed to the steam reforming reaction that converts methane to CO or CO_2 and H_2.

Oxygenated compounds concentrations trend, CO and CO_2, resulted opposite and, in particular, moles of CO increases with increases in temperature, while CO_2 production decreases at 923 K with respect to 823 K. This trend could be attributed to the reformation of CH_4 with CO_2 [23].

As discussed earlier and as clearly showed in Fig. 3, in terms of gaseous products composition, experimental data sufficiently fit with the thermodynamic analysis, especially at 923 K. Therefore, by thermodynamic and experimental investigation it has been possible to reveal that optimal conditions for hydrogen production are: temperature of 923 K, pressure of 1 bar and water to glycerol molar ratio of 9:1. Under these conditions, methane production was very poor and coke formation was minimized, indeed catalytic information has shown stable activity.

On the basis of thermodynamic analyses, products molar fractions of steam reforming process were estimated (Fig. 4), in terms of heat and mass balances, according to industrial biodiesel production cycle (see paragraph 2). In particular, the calculations are based on the starting conditions equal to $T_{in} = 298$ K and $p_{in} = $ constant $= 1$ bar.

From energetic point of view, the steam reforming section has been divided into four distinct sub-modules:

(1) *Crude glycerine purification*: where the crude glycerine, coming from biodiesel production cycle, was reduced of the "poisons fraction" (5 wt.% than total amount of crude glycerine [3]) in order to obtain a chemical composition similar to commercial glycerol: $T_{out} = 563$ K.
(2) *Water vaporizer*: $T_{out} = 373$ K.
(3) Superheater, where the gas stream mixture ($C_3H_8O_3$ and H_2O) is heated to Tr (923 K).
(4) Reformer unit, where the reforming reaction takes place.

To simplify the evaluation of necessary heat for vaporization and heat for overheating, it was considered to provide heat (Eq. (3)) separately to the pure substances in solution. The heat necessary for

vaporization was taken account both sensible heat and latent heat of vaporization of water and glycerol (enclosed into crude glycerol purification sub-module).

$$Q_{vap} = c_p(T_{boil} - T_{in}) + \lambda \tag{3}$$

where c_p is the specific heat at constant pressure in liquid phase, T_{boil} is the boiling temperature of the substance in question, 373 K for water and 563 K for glycerol, and λ is the latent heat of vaporization. The heat required to heat up the substances (Q_{sup}), in the gas phase, from the boiling temperature up to the reaction one ($T_{rea} = 923$ K), was performed as the difference in enthalpy of the substance between the reaction temperature (H_{rea}) and boiling point (H_{boil}) (Eq. (4)):

$$Q_{sup} = H_{rea} - H_{boil} = c_{pm}(T_{rea} - T_{boil}) \tag{4}$$

where c_{pm} is the average specific heat at constant pressure in gas phase between T_{rea} and T_{boil}.

The enthalpy of water at considered temperatures was evaluated using the Mollier diagram. For glycerol in gas phase was necessary to evaluate the specific heat at constant pressure, temperature dependent, through a theoretical equation [24] that simplified for glycerol becomes (Eq. (5)):

$$c_p(T) = a_1(T) + a_2(T)n_C + a_3(T)n_H + a_4(T)n_O \tag{5}$$

where $a_i(T)$ are temperature dependent coefficients [24] and n_C, n_H and n_O are respectively the number of atoms of carbon, hydrogen and oxygen which constitute glycerol molecule. The heat required in reformer section was evaluated by the $\Delta H°r_{SR}$ (Eq. (2)) which expresses the amount of heat absorbed during the reaction.

After determination of absorbed heat amount in each reformer plant section, the thermal power demand of each section (Fig. 4) was calculated as a product between the inlet flow and the heat required for processing. In detail, the calculations have been performed to evaluate the energy and mass balance for this plant section (Purification/Water Vaporizer-Superheater/Reformer), by taking into account that the section should have a capacity to treat 2235 kg h^{-1} of crude glycerine and 3148 kg h^{-1} of water.

As shown in Fig. 4, the calculations evidenced that:

(1) A flow of 3148 kg h^{-1} of additional water have to be supplied to correct S/C ratio (3.0 mol mol^{-1}).

(2) The total energy requested to purify the crude glycerine was 3766 MJ/h.
(3) The net energy requested to vaporize and heat "pure glycerol" and water mixture were 4096 and 11,693 MJ h^{-1}, respectively.
(4) The total energy input to sustain steam reforming reaction at 923 K and 1 bar was 3848 MJ h^{-1}.
(5) The syn-gas outflow produced by glycerol steam reforming is composed of a mixture of CO (387.61 Nm^3 h^{-1}), CO_2 (903.14 Nm^3 h^{-1}), water steam (3033.46 Nm^3 h^{-1}), CH_4 (16.09 Nm^3 h^{-1}) and hydrogen (2597.31 Nm^3 h^{-1}).

At the exit of reforming step, a flow of gas with the composition as above specified, is ready to be treated in the bottoming cycle based on molten carbonate fuel cells.

4. Molten carbonate fuel cells bottoming cycle

4.1. Cycle description

The crucial aspect for having an optimal energy balance for the studied biodiesel production plant concerns the integration of a bottoming cycle for the production of energy through the glycerol decomposition into syn-gas and its use in molten carbonate fuel cells (MCFC) system to produce heat and electricity.

In such a plant lay-out, the best benefits can be obtained if heat and electricity produced by MCFC system will be utilized to meet energy requirements of main production process. Thus, the energy flow balance has been sized to generate electricity as required by the plant (303.6 kW) and heat (31,018 MJ h^{-1}) as much as possible. The syn-gas flow (6937.6 Nm^3 h^{-1}) coming from reformer section is supplied in part (6278 Nm^3 h^{-1}) to an industrial burner and in part (659.62 Nm^3 h^{-1}) to a MCFC system for electricity and heat co-generation. Table 3 reports the flows of each specific gas from exit of reformer process to burner and to MCFC system.

The gas flow and energy balances of the bottoming cycle are detailed in Fig. 5.

From this flow sheet, it is noticeable that MCFC and burner are closely integrated; in fact, the MCFC anode spent gas (119.87 Nm^3 h^{-1}) is recycled to the burner for the combustion of residual hydrogen, carbon monoxide and methane. At the same time, a partial flow of exhausts at the exit of burner is recycled

Table 3
Syn-gas flow rate.

Syngas	Real plant output (Nm^3 h^{-1})	MCFC inlet (Nm^3 h^{-1})	Burner inlet (Nm^3 h^{-1})
CO	387.61	36.85	350.76
CO_2	903.14	85.87	817.27
H_2O	3033.46	288.42	2745.04
H_2	2597.31	246.95	2350.36
CH_4	16.09	1.53	14.56

Table 4
MCFC operative parameters.

H_2 consumption (Nm^3 h^{-1})	165.46
H_2 flow rate (Nm^3 h^{-1})	246.95
H_2 utilization (%)	67
Voltage (V)	276.30
Power (kW)	303.6
O_2 consumption (Nm^3 h^{-1})	82.78
O_2 flow rate (Nm^3 h^{-1})	275.96
O_2 utilization (%)	30
CO_2 utilization (%)	30.08

to supply MCFC inlet cathode with the necessary flow of CO_2 (550 Nm^3 h^{-1}).

4.2. MCFC and burner energy balances

The bottoming cycle has been conceived with two main subsystems: the MCFC system, operating as electricity generator, and the burner, operating as heat generator.

The molten carbonate fuel cells system concerns a series of stack operating at 923 K of temperature and fed by a flow of syn-gas. In this evaluation, MCFC system has been selected for several reasons: (i) commercial availability, even if at a demonstrative level; (ii) MCFC technical features well fit with plant requirements; (iii) MCFC can be directly supplied by syn-gas and the high operative temperature makes outlet gases an useful thermal vector.

In our plant scheme, the MCFC system is supplied by a flow, F_{sfc}, of 659.62 Nm^3 h^{-1}, with the composition as detailed in Table 3, who gets a combustion potential of: P_{in} = 894.76 kW.

A commercial MCFC system suitable for this application presents an operative balance as specified in Table 4.
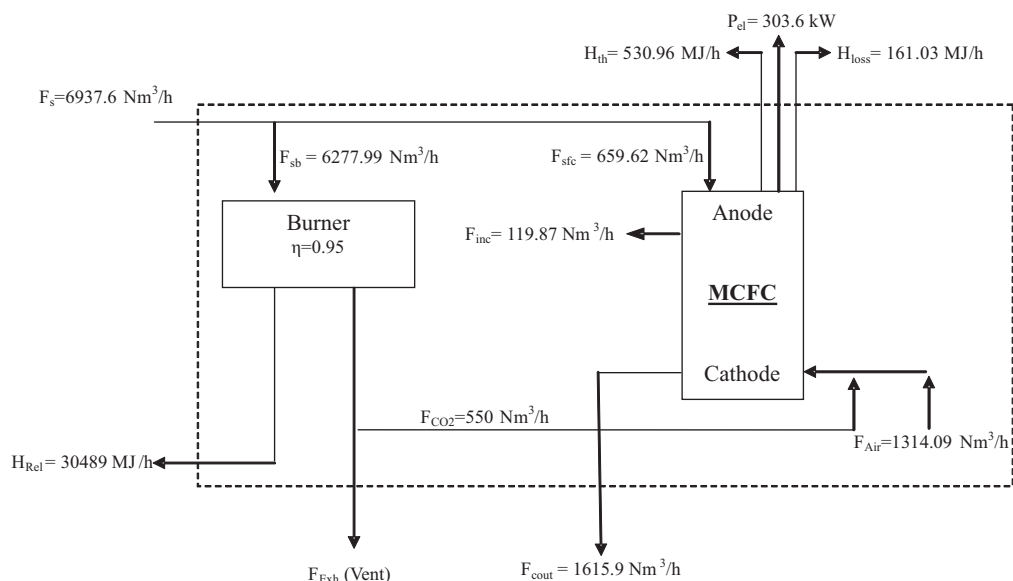

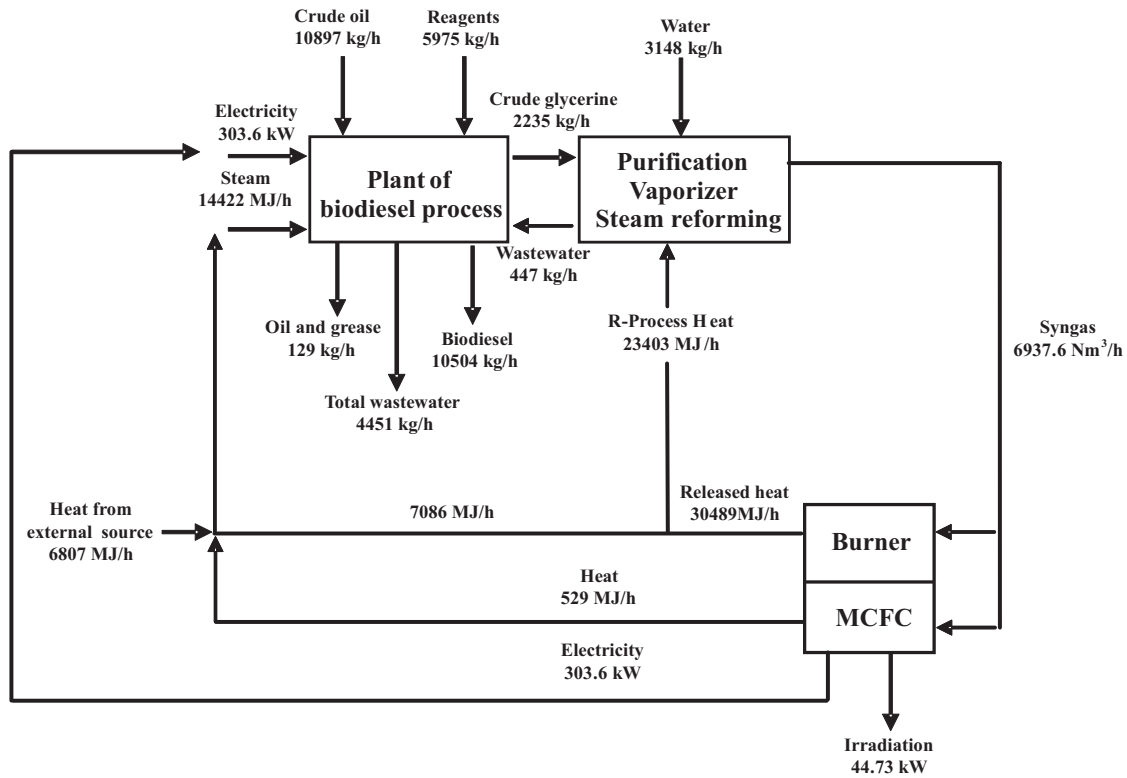**Fig. 5.** Gas flow and energy balance of bottoming cycle.

Fig. 6. Mass and energy flows for the global process.

Under a general point of view, the MCFC energy balance can be defined with the Eq. (6):

$$P_{in} = P_{el} + H_{loss} + H_{inc} + H_{th} \qquad (6)$$

where P_{el} is the released electric power (303.6 kW); H_{loss} is the heat loss due to irradiation, prefixed equal to 5% of inlet energy flow (44.73 kW); and H_{inc} is the potential energy of combustion available in the outlet MCFC exhaust (398.94 kW), based with respect to LHV.

By developing the above reported equation, it has been determined the heat flow H_{th} = 147.49 kW (529 MJ h^{-1}) released by MCFC, as sensible heat, and the MCFC electricity efficiency has been calculated with Eq. (7):

$$\text{MCFC el. eff.} = \frac{P_{el}}{P_{in}} \times 100 = \frac{303.6}{894.76} \times 100 = 33.9\% \qquad (7)$$

The combustion section concerns a burner with a potentiality to treat an inlet flow of syn-gas (6277.99 Nm^3 h^{-1}) plus a flow of exhaust gas (119.87 Nm^3 h^{-1}) recycled from MCFC anode compartment.

The thermal power released by the burner has been calculated on the basis of lower heating value and a burner efficiency of 95%.

From this calculation it is noticeable that thermal power generated by this section is equal to:

$$H_{Rel} = 8469.29\,\text{kW} = 30{,}489\,\text{MJ h}^{-1}$$

The thermal power available from the combustion of gases produced by glycerol steam reforming corresponds to a rate of 80.6% of the total heat requirements (main process/vaporizer/reformer/bottoming cycle).

In addition to this one, a partial flow of combusted exhaust at exit of burner is recycled to MCFC cathode compartment to supply CO_2 requirements.

Table 5
Input/output products.

Product	Source	Input	Output
Soybean oil		10,897 kg h^{-1}	
Reagents		5975 kg h^{-1}	
	Burner	30,489 MJ h^{-1}	
Heat	MCFC	529 MJ h^{-1}	
	External source	6807 MJ h^{-1}	
Electricity	MCFC	303.6 kW	
Irradiation			44.73 kW
Biodiesel			10,504 kg h^{-1}
Oil and grease			129 kg h^{-1}
Total wastewater			4451 kg h^{-1}

5. Conclusions

The investigation on the theoretical feasibility of a process plant, devoted to the production of biodiesel, integrated to a subsystem for the production of electricity and heat from glycerol, generated as by-product of the main process, has been successfully performed. A mathematical model has been developed to determine energy and mass balance of vaporizer/reformer/bottoming cycle. The calculations have been validated by comparison with a set of experimental results.

The overall mass and energy balance of the whole process has been determined as shown in Fig. 6, while Table 5 summarizes input and output of the global process in terms of materials and energies.

The comparison of this flow-sheet with a traditional one evidenced that:

- Inlet mass flows of crude oil and chemicals do not change as well as amount of produced biodiesel, with the exception of glycerol that in traditional production line appears as by-product while in the proposed scheme is treated to sustain energy requirements of main process.

- Traditional plant (in the examined size) requires electricity (303.6 kW) and heat (14,422 MJ h^{-1}) from external sources, while the proposed process requires a reduced rate (6807 MJ h^{-1}) of heat from external.
- The plant integrated with bottoming cycle shows a self-production of energy of 82.5%, with a substantial enhancement of plant complexity, that should require a further analysis how it influences plant cost investment.

References

[1] J. Sheehan, V. Camobreco, J. Duffield, M. Graboski, H. Shapouri, "Life Cycle Inventory of Biodiesel and Petroleum Diesel for Use in an Urban Bus", NREL/SR-580-24089 UC Category 1503, National Renewable Energy Laboratory, Golden, CO, 1998.
[2] S. Adhikari, S.D. Fernando, A. Haryanto, Energy Convers. Manage. 50 (2009) 2600–2604.
[3] J.C.J. Bart, N. Palmeri, S. Cavallaro, "Biodiesel science and technology; From soil to oil" Woodhead Energy Series N. 7 (2009).
[4] S. Douvartzides, F. Coutelieris, P. Tsiakaras, J. Power Sources 131 (2004) 224–230.
[5] S. Douvartzides, F. Coutelieris, A.K. Demin, P. Tsiakaras, AIChE 49 (2003) 248–253.
[6] F. Frusteri, S. Freni, J. Power Sources 173 (2007) 200–209.
[7] G. Maggio, S. Freni, S. Cavallaro, J. Power Sources 74 (1998) 17–23.
[8] S. Cavallaro, V. Chiodo, A. Vita, S. Freni, J. Power Sources 123 (2003) 10–16.
[9] V. Chiodo, S. Freni, A. Galvagno, N. Mondello, F. Frusteri, Appl. Catal. A: Gen. 381 (2010) 1–7.
[10] N. Palmeri, V. Chiodo, S. Freni, F. Frusteri, J.C.J. Bart, S. Cavallaro, Int. J. Hydrogen Energy 33 (2008) 6627–6634.
[11] W. Du, W. Li, T. Sun, X. Chen, D. Liu, Appl. Microbiol. Biotechnol. 79 (2008) 331–337.
[12] R. Garofalo, EU Biodiesel Potential Defining the Opportunities, Roundtable on Sustainable Biofuels Consultation: Europe Stakeholders outreach meeting, Belgium, 2009.
[13] M. Balat, H. Balat, Energy Convers. Manage. 49 (2008) 2727–2741.
[14] European Biodiesel Board, "EU biodiesel industry shows resilience amid unfair international competition and degraded market conditions", 689/COM/09 (2009).
[15] B. Freedman, E.H. Pryde, T.L. Mounts, J. Am. Oil Chem. Soc. 61 (1984) 1638–1643.
[16] F. Ma, M.A. Hanna, Bioresour. Technol. 70 (1999) 1–15.
[17] R. Jens, Rostrup-Nielsen, J.R Anderson, M. Boudart, "Catalytic Steam Reforming" - Catalysis Science and Technology, 1983.
[18] S. Adhikari, S. Fernando, A. Haryanto, Renew. Energy 33 (2008) 1097–1100.
[19] S. Adhikari, S. Fernando, S.R. Gwaltney, S.D. Filip To, R.M. Bricka, P.H. Steele, A. Haryanto, Int. J. Hydrogen Energy 32 (2007) 2875–2880.
[20] X. Wang, S. Li, H. Wang, B. Liu, X. Ma, Energy Fuels 22 (2008) 4285–4291.
[21] A. Iriondo, V.L. Bario, J.F. Cambra, P.L. Arias, M.B. Guemez, R.M. Navarro, M.C. Sanchez-Sanchez, J.L.G. Fierro, Top Catal. 49 (2009) 46–58.
[22] I.N. Buffoni, F. Pompeo, G.F. Santori, N.N. Nichio, Catal. Commun. 10 (2009) 1656–1660.
[23] A.N. Fatsikostas, D.I. Kondarides, X.E. Verykios, Catal. Today 75 (2002) 145–155.
[24] R.H. Perry, D.W. Green, "Perry's Chemical Engineers Handbook", 7th ed., 1998, ISBN: 0071159827.